CRANIOFACIAL TISSUE SIMULATION USING CONTACT ANALYSIS OF THE FINITE ELEMENT METHOD

Unaizah Obaidellah[1], Zati Azizul[2], Erma Rahayu Mohd Faizal[3], Ram Gopal Raj[4]

[1,2,3,4]Department of Artificial Intelligence, Faculty of Computer Science and Information Technology, University of Malaya, 50603, Kuala Lumpur, Malaysia

[1]unaizah@um.edu.my, [2]zati@um.edu.my, [3]erma@um.edu.my, [4]ramdr@ um.edu.my

ABSTRACT

A corrective surgery known as the craniofacial surgery is important for the improvement of a patient's appearance and in some cases a patient's physical abilities in terms of speech. The postoperative soft tissues prediction is often a hit considering the complex facial anatomy. Such surgical planning may be made simpler and more precise with the use of computational modelling of the relevant area. This paper presents a general framework for the simulation of soft tissue in order to predict the postoperative results of maxillofacial surgery based on the finite element method. Methods for the facial model preparation used in the analysis are described. A 3D facial model of the facial skin and the underlying lower jaw is modelled from a patient-specific CT data. In conjunction with the representation of soft tissue mechanical properties and boundary assignment, the models were submitted for a contact analysis for a computational postoperative appearance. Finally the simulation results are shown for the case study data.

Keywords: Finite element modelling, craniofacial surgery, soft tissue simulation, surgery planning, biomechanics

1.0 INTRODUCTION

Aesthetic aspects such as perceived individual beauty are often determined by the appearance where even a slight facial malformation may influence one's impression of an individual [1][2][3]. Moreover, the face has a considerable role in performing functions such as breathing, eating and talking. Thus, an individual suffering from facial deformities due to a family trait or trauma may experience low self-esteem and difficulties performing these basic functional systems [4][5]. Therefore, the treatment of these abnormalities aimed at improving the functionalities and the reconstruction of proportioned aesthetics is important [6]. Given the complexity of predicting a harmony appearance that a surgeon may encounter prior to the actual surgery of a particular patient, the use of a computer system [7][8] is deemed beneficial for this purpose.

This paper describes the underlying mechanism for the prediction of a face based on the soft tissue simulation for the *orthognathic* surgery using the contact analysis of the finite element modelling. This system incorporates the bone structure models with the soft tissue models to predict soft tissue changes as a result of the bone realignment. This exploratory study introduces a preliminary prototype system that consists of two components; facial modelling and numerical computation. The facial surgery planning of this system such as the lower jaw advancement for the realignment with the upper jaw is numerically computed using the linear elastic analysis of the finite element method. This is achieved by employing various sequential image processing techniques to produce a simplified anatomical representation defined with appropriate biomechanical properties that closely characterizes the real face.

For the purpose of this work, the facial model used is reconstructed from volume scans CT images of an actual and individualised patient data where a tissue segmentation technique is utilised to classify tissue types that range from the internal layer of the skull to the external skin. In theory, using data from actual facial models on a finite element platform is beneficial since ground-truth data is favourable in accessing the quantitative evaluation. However, due to the complexity of the human facial anatomy, facial models derived from actual data are usually simplified by considering the most vital information such as the skull and the skin layer. Following this, advanced craniofacial anatomy such as the facial blood circulation, nerves and muscle anatomy are not considered in this work.

This paper makes the following contributions to the discipline:

- *The use of real patient data to model the facial anatomy*
  In previous reports particularly in facial animation [9][10][11][12], template based face data are commonly employed instead of actual data sets. These generic face templates are chosen depending on the skull similarities or properties such as ethnicity, gender and age. Consequently, the skin layer is mapped on the generic model template, thus, the facial appearance deformation is estimated based on the interpolation of the corresponding landmark points of the model skull and the target skull. The limitation of such procedures is that the predicted results would be incorrectly biased according to the chosen template as unwanted facial appearance is adopted in the final predicted results. In addition, the use of the template-based model produces an unspecific reconstruction as the prediction is not performed based on an individualised data set. For this reason, a patient specific surface based model obtained from tissue segmentation is used to initiate the craniofacial surgery simulation [13][14][15]. By means of the finite element analysis, the deformation to the facial anatomy can be predicted through the interpolation of the prescribed deformation.
- *The use of contact analysis*
  The derivation of tolerable simplified model is important in this work. To achieve the contact analysis, the soft tissue simulation is computed by means of the rigid lower jaw acting towards the elastic deformable facial skin. This is similar to the standard surgical procedure where movements of the bones (rigid body) have a direct affect to the elastic surface (deformable body). Various attempts with different material parameters and boundary conditions are carried out during the model set-up to determine the optimised chosen approach of contact analysis for the model.
- *The use of linear finite element analysis*
  In general, non-linear elastic approach is more suitable to cater for large soft tissue deformation [15][16][17][18][17] on a finite element platform. However, the linear elastic approach is still an alternative when dealing with smaller living tissue deformation such as the case in this work. The advantage is that the technique reduces the computational costs yet still yields a successful simulation of complex soft tissue deformation.
- *Static soft tissue prediction*
  This paper predicts the result that is considered as static with attention given to the first impression of the patient's postoperative facial appearance, instead of the estimation of patient's facial mimic due to muscular activity which is defined under the dynamic soft tissue prediction. In order to resemble the actual tissue behaviour as precise as possible, the 3D facial model is assigned with appropriate material and properties values.

This paper begins by considering the problems of representing a realistic facial model in section 2. Section 3 presents the methods of producing a realistic 3D model in preparation for the soft tissue simulation, section 4 presents the results of the predicted facial soft tissue simulated based on the contact analysis. Lastly, section 5 draws some conclusions and recommendations for future work.

2.0 BACKGROUND AND PREVIOUS WORK

The development of advanced computer graphics, simulation and computing hardware has accelerated the study on three-dimensional medical imaging enabling a more interactive and convincing prognosis between the clinicians and the patients. Three-dimensional (3D) medical imaging is a tool that allows clinicians to view 3D representation of anatomic structures on a computer screen promising enhanced visual representation, diagnosis and treatment planning for various physical disorders in medicine including orthognathic surgery and orthodontic treatment in dentistry. Several types of modalities such as conventional tomography [19][20], computer tomography (CT) [21][22], magnetic resonance imaging (MRI) [23][24] and ultrasound [25] are available in the 3D medical imaging by producing a set of sequential cross-sectional slice images of the human body. Across these types of modalities, CT is often accepted as the best modality used to filter hard tissue data, while MRI is excellent for soft tissue representation [26]. CT images are achieved by direct but minimal x-ray radiation to the body part of concern by a few scanning components comprised of a detector array, an x-ray source, a patient support couch and a computer featured with suitable operating console. During scanning, a thresholding process separates diverse tissues such as bone, teeth and skin for improved visualization for the tissue structure of interest. This is achieved by defining a specific range of gray values which classifies these tissue structures. The idea of soft tissue prediction is initiated as a result of the underlying bone realignment [27]. In effect, the growth of the craniofacial surgery systems has been remarkable [28][29][30]. Various numerical methods have been used in the physical-based modelling such as the simulation of soft tissue deformation. The two common approaches are the mass-spring-model and finite element method.

The mass-spring-model uses a technique that consists of a collection of point masses, connected by springs in a lattice structure that applies forces on its neighbouring points as the mass displaces from its current position. The mass-spring systems have been frequently used in the simulation of multi-layer skin model incorporating the simulation of muscle deformation. Terzopoulos and Waters [9] used three mass-point mesh layers to respectively represent the dermis, subcutaneous tissue and muscle of the facial tissue. Lee and Terzopoulos [31] improved the approach by employing constraints to prevent penetrations between soft tissues and bone. A more advanced simulation incorporating the muscle deformations were tested by [32] where muscle shapes were changed in its form under the influence of the mass-spring mesh. Further, in effort to include the soft tissue material properties on their anatomy models, [33] offered control over isotropy or anisotropy of elastic material. The mass-spring systems are advantageous at constructing interactive and real time simulation within a short period of time on typical desktop systems. This is because mass-spring systems use less complex mathematical formulation of Newton's motion equation [13] where each node is given a differential equation of second degree depending on the mass, damping and sum of all spring forces influencing the system [34]. Therefore, less computation is required for the completion of a successful analysis. However, although this method is ideal for large displacements and deformation, the technique is less reliable as the physical properties of the human tissue are handled in terms of spring constants. Due to the reason that mass-spring models are handled in terms of spring constants, values and constraints to be assigned to these constants are not easily distributed. Another known problem appeared when spring constants are large. Large constants are used to model rigid or non-penetrable models. Therefore, deformations results are difficult to achieve if small time steps for numerical computation resulted in slow simulation [35] are not applied.

The finite element method proposes a more realistic simulation [13][36][37]. In the finite element method, an object is considered a continuum, meaning a solid body with mass and energies distributed throughout the object in consideration. The continuum is divided into a finite number of elements joined at node points. In order to obtain deformation of the object, a combined function that solves the equilibrium equation found for each element is solved.

The facial appearance is simulated based on the finite element method by cutting and stretching the skin rather than considering the underlying bones repositioning [38]. At another level, the postoperative appearance acquired from both the mass-spring and finite element models is compared [36]. However, the study used a generic facial mesh to map the general anatomical structure to the individual patient data. In order to produce visually appealing facial surface, the prismatic functions of C^1 continuity on the patient-specific 3D facial surface, in a non-linear approach, which is connected to the bone structure using the C^0 continuous function is employed [39]. Employing volumetric tetrahedral grids, the outcome produced by [15][17][40] differ in terms of surgery planning in accordance to the guidelines appropriate for a patient-specific functional rehabilitation under the supervision of craniofacial surgeons. Their approach lacks sufficient material models to represent biological tissues. More recently, a postoperative soft tissue simulation has been proposed using the muscular anatomy [41].

The model presented in this paper proposes a methodological approach of predicting the soft tissue appearance using the finite element method by employing the contact analysis on a patient-specific facial model based on the featured underlying bone realignment surgical specification. The primary benefit of our model apart from the availability of the simulation of post-operative results is that the soft tissue deformation under stress and strain can be simulated and the simulation can also be viewed at any given time frames.

3.0 METHODS

3.1 3D Facial Modelling

Preparation of the 3D facial model for the finite element analysis is divided into several stages as shown in Fig. 1 below.

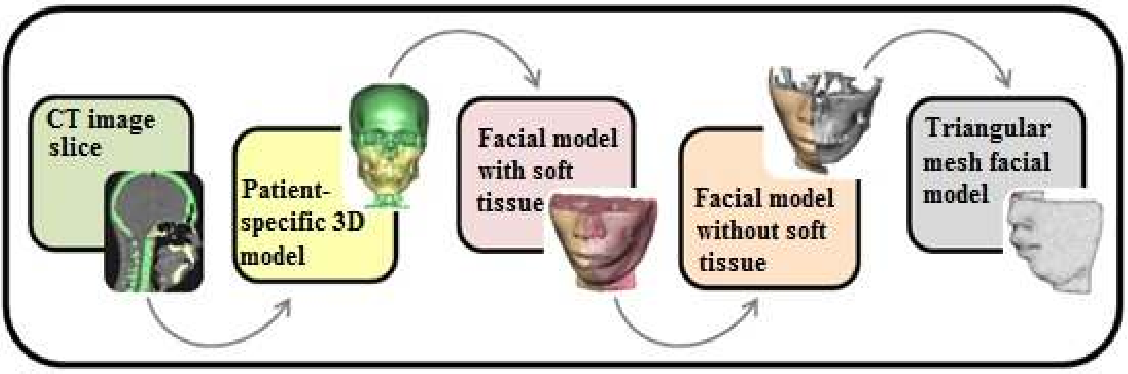

Fig. 1: The sequence of the 3D generation of the facial model

a) Image segmentation

A patient-specific 3D facial model is reconstructed from the computer tomography (CT) data using the Marching Cube Algorithm [42] that specifies the region of interest and adjusts the contrast of the images. The simplified 3D models generated in this work consist of the upper jaw, lower jaw and the facial skin surface, each represented by triangular meshes as they are the most primitive shape for 2D elements. A mesh is defined as the partitioning of geometry into simple small elements such as triangles or quadrilaterals. The models which were reconstructed at different stages require the CT images to be segmented based on the region of interest by specifying a lower and upper threshold value. The lower values used were 226 and -774, while the upper values were 352 and -5, respectively for the bone and skin. These values highlight the desired regions on the CT image slices for the construction of the 3D facial models. These 3D models are constructed from the CT images based on the conversion of pixel-based images to a triangular mesh using special medical image segmentation software, Mimics [43]. This process known as triangulation may include unwanted parts. Therefore, manual editing that removes the excessive threshold pixel to clean the models is crucial to eliminate the unnecessary facial regions.

b) Pre-processing prior to model construction

These facial models are triangulated using the STL interface that generates a triangle mesh around the volume where each surface pixel from the segmented CT image produces two triangles. A number of pre-processing procedures were performed to produce an ideal model that compromises between the computer time and the quality of the STL format.

<u>Methods of interpolation</u>

Interpolation is a technique applied during the triangulation to determine the level of quality for the models. The two types of interpolation are called the contour and grey interpolations. The contour interpolation is a 2D interpolation in the plane of the images that is expanded to the third dimension. On the other hand, the grey interpolation that accounts the partial volume effect by considering the previous and following image during an interpolation produces accurate model construction. However, this includes the unnecessary details due to noise from the CT images, thus, does not always produce good quality models. This is because the produced mesh gives a noisy surface when a slice distance of the scan considerably deviates from the slice thickness, a condition that relies on the data acquisition during the scanning process. Therefore, the contour interpolation is opted as it gives smoother 3D results with reduced gaps. The following Fig. 2 shows a visual comparison between the contour and grey interpolations.

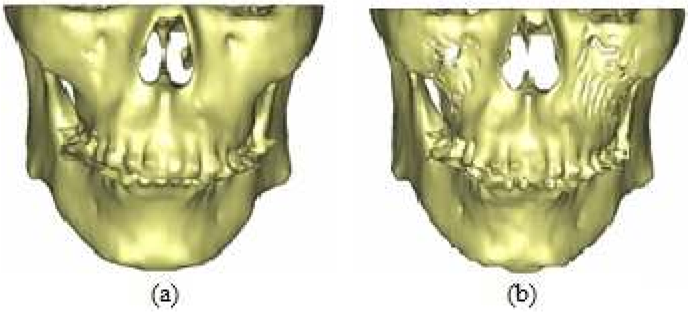

(a) (b)

Fig. 2: Methods of interpolation. (a) Contour and continuity, and (b) Grey with the continuity and accuracy matrix reduction option

Matrix reduction

Prior to triangulation, voxels (or pixels in 3D) are grouped according to the XY plane and Z direction. The X and Y planes refer to the size of a pixel, while Z direction for the height. A larger value assigned to each size and height of a pixel produces a smaller voxel count for the model that indicates reduced information, which leads to less accurate results. The two types of matrix reduction algorithm are the accuracy and continuity. The accuracy algorithm produces appealing model dimension. However, these produces lower quality models as gaps appear when the wall thickness of the model appears smaller than the pixel size. In contrast, the continuity algorithm was preferred due to the better quality model dimension produced when bigger matrix reduction is adopted.

Triangle reduction

In order to ensure optimum mesh on the models for the intended finite element analysis, the following pre-processing analysis aims at producing equilateral triangles. This means each triangle are characterised to have an equal length with 60 degrees at every angle. Judgement of a good mesh relies on the small elements for details, large elements for efficiency or/and nicely shaped elements for accuracy. However, there is a trade off between the elements shape and the computational resources for the analysis where elements with more sides and more complex shapes are likely to increase the computational time to produce a solution during an analysis. The quality of a triangle is measured by normalizing the ratio between the height and base value of the triangle. Lower quality triangles that do not satisfy this condition are either eliminated or improved by reshaping existing triangles. Fig. 3 (a) and (b) shows an example of low quality mesh model called *mesh cobwebs* contains many small triangles shown by dark spots on the geometry. During this mesh optimization process, a few elements may potentially intersect as shown in Fig. 3 (c). This is fixed by the manual operation of deleting the intersected elements and recreating them by patching the affected area with newly created triangular elements.

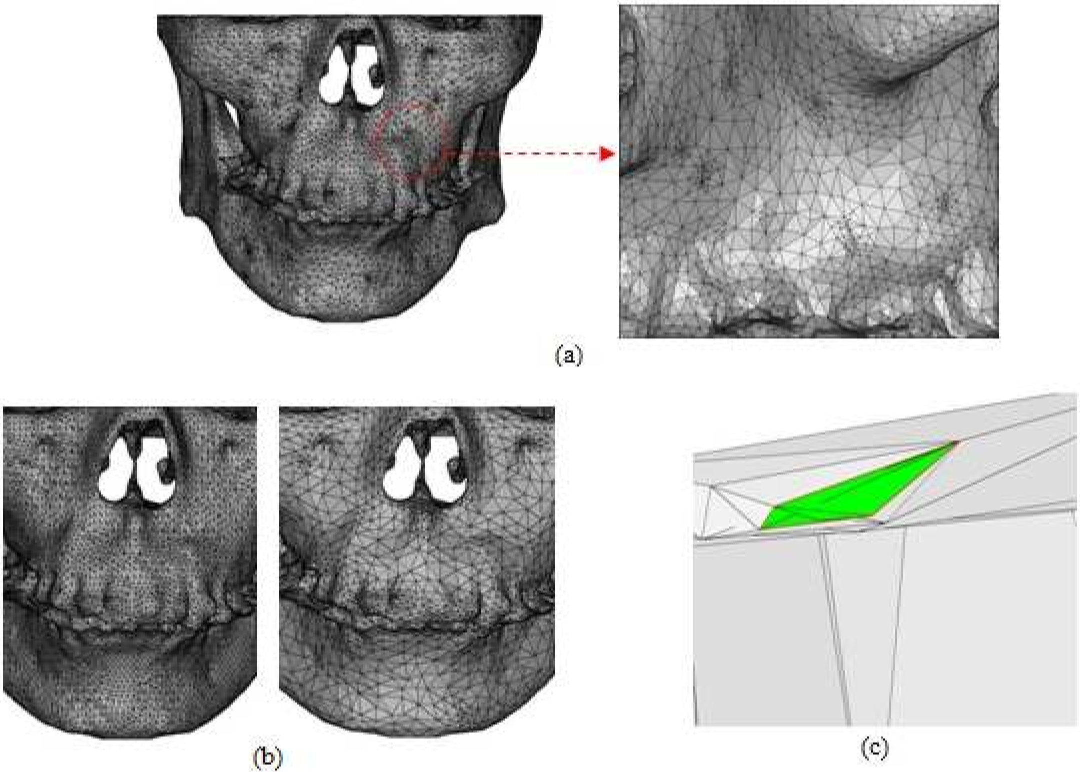

Fig. 3: (a) Mesh cobwebs. (b) Before (left) and after (right) triangle reduction.
(c) An example of intersecting triangles

Smoothing

The models are further submitted to the following pre-processing stage called smoothing that filters lower quality elements to make rough surfaces smoother. This process is crucial as any models with rough surfaces will impede a successful analysis. Furthermore, sharp regions such as the area around sharp teeth are not easily meshed, thus, increases the potential of mesh cobs. Therefore, the rough surfaces are smoothed by deleting and recreating new sets of triangular elements as shown in Fig. 4.

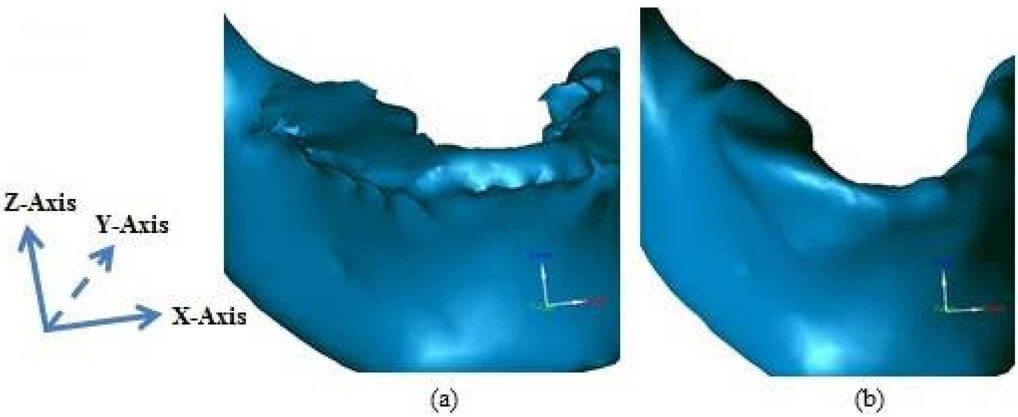

Fig. 4: Improved mandible structure. (a) Rough surface mandible,
and (b) smoothed surface mandible

c) Bone cuts

The aim of this research is to predict the post-operative appearance using the contact analysis approach of the finite element analysis. The prediction is done by simulating the underlying bone cuts. The procedure for the bone cut and repositioning called *osteotomy* are modelled according to the patient-specific medical specification as shown in Fig. 5. The case study used in this research emphasise on the advancement of the lower jaw that was realigned with the upper jaw. In effect, this would predict the facial appearance for this particular patient. Fig. 5 (b) and (c) shows the differences between the forwarded lower jaw to the upper jaw before and after the osteotomy procedure. The amount of translation and rotation are recorded as input for the analysis. These were used to compute the displacement vector for each node that replicates the intended movement during surgery.

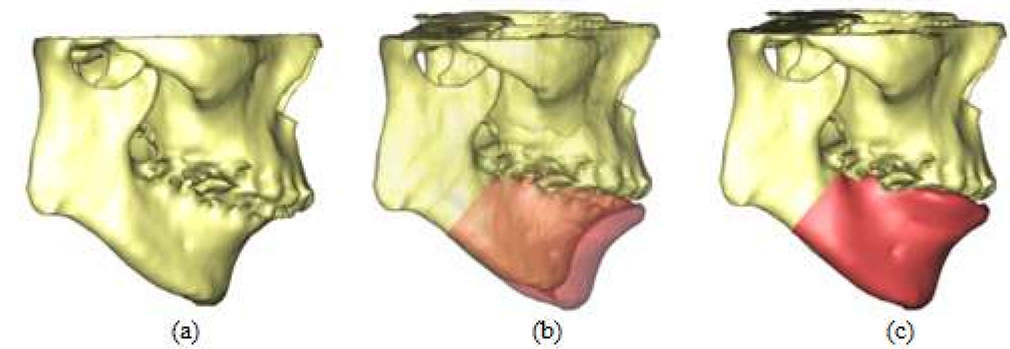

Fig. 5: The osteotomy simulation. (a) Pre-operative bone structure, (b) sliced lower jaw that is relocated to a new position, and (c) post-operative bone structure

3.2 Finite element analysis

A number of assumptions were considered to achieve the required computation efficiency. Apart from that described, advanced facial tissues such as muscular anatomy, fat and water were not incorporated due to insufficient anatomical information, excessively complex computation and lack of available system memory for the completion of an analysis within a reasonable time frame.
The finite element method is an approach that divides a system into a large number of small elements where cells interact between adjacent units, thus imitates the physical reality. The employed numeric methods find the deformation of the physical structure under predefined boundary conditions such as loads or forces. The use of finite element analysis is due to the benefit of limiting errors in the computations, the ability to account for different material properties as well as the simplified depiction of the complete system, in this case, the face.

a) Quadrilateral mesh generation

The post operative appearance simulation can be acquired by analysing the coupled interaction between the rigid bones and the underlying skin layer. At the initial point of analysis, both of these models are separated as they are not in contact with each other. Thus, a variation of the finite element analysis called the contact analysis that will be described is modelled necessitating the use of quadrilateral, rather than the triangular meshes. A single quadrilateral element consists of four sides and four vertices.
A new mesh region is created based on the existing triangular surface models where the number of quad elements is calculated based on the ratio between the longest geometry edge length and the global edge length of each element. A small global edge length value that produces a high density mesh due to excessive detail is compromised so long sufficient facial model information is sustained. Upon completion of the conversion, the models are checked to ensure all elements are tied with each other before any

duplicated elements are removed. This is because the accuracy of an analysis is primarily dependant on the quality of the mesh. Further verifications including tests on nodes connectivity, elements duplication, and quality of the element shapes are performed.

b) Material properties

On completion of these tests, the models composed of finite number of elements are defined with appropriate material properties such as stiffness, density and elasticity. Assuming that the skin surface layer is *isotropic* and *homogeneous*, these properties are modelled using the constitutive equations. The elasticity nature of the skin [44] calls for the use of the elastic model which describes the linear relationship between stress and strain producing the Young's modulus, E

$$E = \sigma/\varepsilon \quad (1)$$

The axial elongation of a structure is accompanied by lateral contraction with the ratio for the linear elastic material called the Poison's ratio, v. The isotropic state where elastic properties are identical in all directions consist of two independent constants which are described as the modulus of rigidity are the shear modulus, G

$$G = E/(2(i + v)) \quad (2)$$

and the Lamé constants, λ

$$\lambda = v\mathrm{E}/((1 + v)(1 - 2v)) \quad (3)$$

These constants derive the isotropic linear elastic material governed by

$$\sigma_{ij} = \lambda\delta_{ij}\varepsilon_{kk} + 2G\varepsilon_{ij} \quad (4)$$

where σ_{ij} is shear stress in $_{ij}$ plane, δ_{ij} is Kroneker delta, ε_{kk} is normal strain parallel to kth axis and ε_{ij} is shear strain in $_{ij}$ plane. The homogeneous material equations which define the stress-strain relationship of those elements that are made of a single material are represented by:

$$\begin{Bmatrix} \sigma_x \\ \sigma_y \\ \tau_{xy} \end{Bmatrix} = \frac{E}{1-v^2} \cdot \begin{Bmatrix} 1 & v & 0 \\ v & 1 & 0 \\ 0 & 0 & \frac{(1-v)}{2} \end{Bmatrix} \cdot \begin{Bmatrix} \varepsilon_x \\ \varepsilon_y \\ \varepsilon_{xy} \end{Bmatrix} \quad (5)$$

c) Allocation of the boundary conditions

The behaviours of a model are often acquired as a response from a particular action(s) such as pressure or loads. These behaviours are also constrained by certain conditions termed as the boundary conditions. An example of a boundary condition in engineering is an end of a cantilever beam fixed to a wall. These criteria are crucial for the finite element analysis as the exclusion would leave the model floating during the computation. Thus, the displacement condition is associated with a sparse number of elements on the skin facial model serving as a constraint for the model from moving in space during the analysis. The boundary conditions of the nodes are specified on the boundary of the body as:

$$\begin{bmatrix} K_{uu} & K_{us} \\ K_{su} & K_{ss} \end{bmatrix} \begin{bmatrix} a_u \\ a_s \end{bmatrix} = -\begin{bmatrix} f_a \\ f_r \end{bmatrix} \quad (6)$$

Where a_u are the unknown nodal values, a_s are the specified nodal values, f_a are the applied nodal loads and f_r are the nodal point reactions. Therefore the solution becomes:

$$a_u = -K_{uu}^{-1}(f_a + K_{us}a_s) \quad (7)$$

$$f_r = -(K_{su}a_u + K_{ss}a_s) \quad (8)$$

The translational and rotational values set to zero for all x, y and z directions indicate that no translational and rotational movement occur from any directions for the specified nodes of each element. Another constraint assigned to the facial models is called contact, with the lower jaw defined as rigid while the skin model as deformable due to the higher degree of stiffness and density of the bone in contrast to other soft tissue materials such as the skin. Relying on this fact, it was assumed that no deformation occurred on the bone although in actuality, all types of material deforms under the influence of a given load.

3.3 Contact Analysis

Normally a Lagrange multiplier is sufficient to calculate the constraint between contacting bodies in virtual reality. However, the basis of a Lagrange multiplier which solves simultaneously the displacement (u) and the Lagrange multiplier (λ) often results in a zero in the diagonal matrix. This leads to a non-positive definition for complex problem such as the one proposed in this paper. Also, there is no mass associated with the Lagrange multiplier degree of freedom. For this reason, the model proposes the use of a direct-constraint procedure to analyse the contact between the rigid surface of the bone and the deformable body of the skin. In the beginning, a target node on the deformable body is initialized with no constraint while contact does not occur. Once contact is detected, the degrees of freedom are transformed to a local system and a constraint is imposed such that

$$\Delta u_{normal} = v \cdot n \quad (9)$$

where v is the prescribed velocity of the rigid surface. This local transformation is continuously updated to reflect the sliding of a point on the deformable body along the rigid surface. Point A in Fig. 6(a) illustrates this sliding effect.

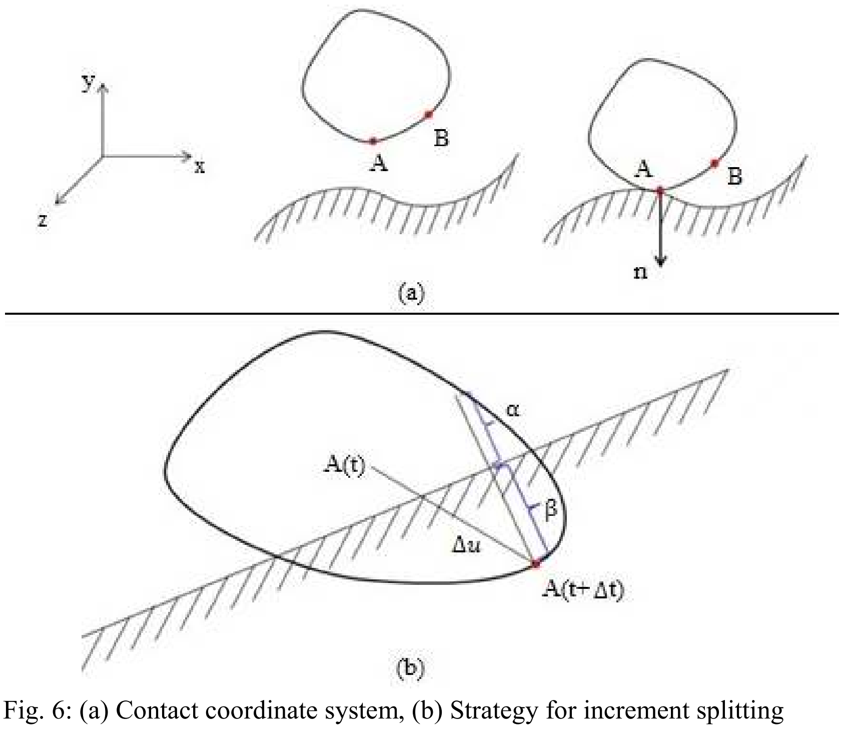

Fig. 6: (a) Contact coordinate system, (b) Strategy for increment splitting

In calculating the displacement between the bone and the skin, it is important to determine when they contact each other and the value of the normal vector at the point of contact. To solve this problem, the model fixes the time step Δt into two periods or subincrements. The first subincrement removes any constraint on node A such that its movement is not obstructed. However, constraint is defined on node A in the second subincrement. By linearizing the displacement increment, the model is able to calculate the time period when contact is first imposed also when penetration is about to occur between the two bodies.

When a node from the bone contacts one from the skin, a tying relation is formed between them. The relation determines the transformation and displacements imposed for each pairing node. With the knowledge of the time increment Δt^{α} and $\Delta t^{\beta}$and the surface velocity (v) known, the configuration of the surface at the end of the increment can be calculated. Since the constraint relationship requires information to the normal of the rigid surface, the distance from the node starting position to the current one is determined as the appropriate normal displacements to be imposed. The normal displacement puts the node at the end of the increment in the same surface segment which is also used to determine the transformation matrix between the local and the global coordinates.

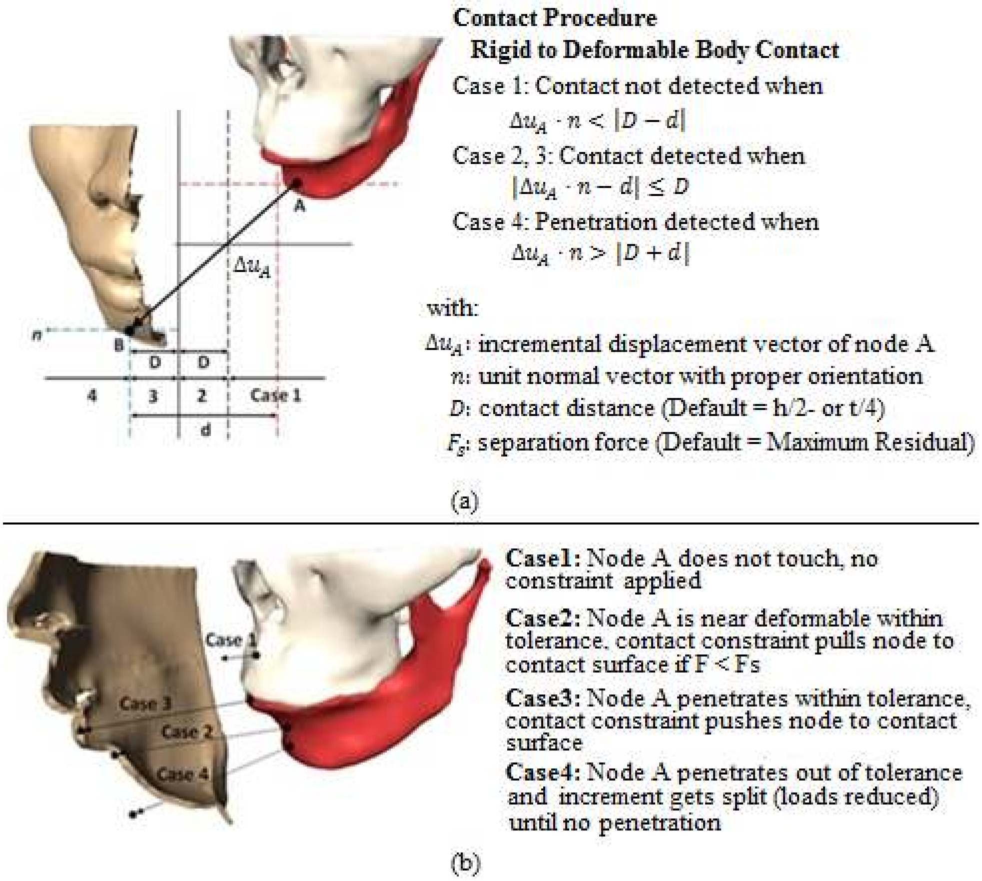

Fig. 7: (a) Rigid and deformable contact definition, (b) description of the four contact cases on the 3D facial model

The deformation of the skin layer is often the results of the forward movement of the mandible, performed according to a motion control with -30 degrees of freedom velocity in the y-direction as a result of the *osteotomy* planning. The negative sign indicates that the contact from the lower jaw acts towards the skin model in a straight and forward direction. At the initial model position, no contact is detected at all between these models as nodes around the boundary of either the lower jaw or skin are not within the contact region. However, during the analysis, nodes belonging to the lower jaw displaces closer to the skin at every iteration. The models are considered contacting with each other once the relocating nodes of the lower bone reaches the deformable skin region called the contact tolerance. The region of the contact tolerance is taken as 5% of the smallest element side and 25% of the smallest element thickness detected around the facial skin model. This is to avoid penetration between these tissues. Hence, the bodies between these models are defined as touching during the analysis setup. Fig. 7 shows the contact definition for the rigid and deformable bodies.

4.0 RESULTS & DISCUSSION

A number of tests were performed on artificial models before the actual facial models were incorporated. These experiments were necessary to compare simulation results to the finite element theory and to validate the advance modelling method on simpler 3D geometry objects. The first test performed to produce an ideal mesh relative to the dimension of the models shows that the number of elements contained in a model determines the deformation accuracy.

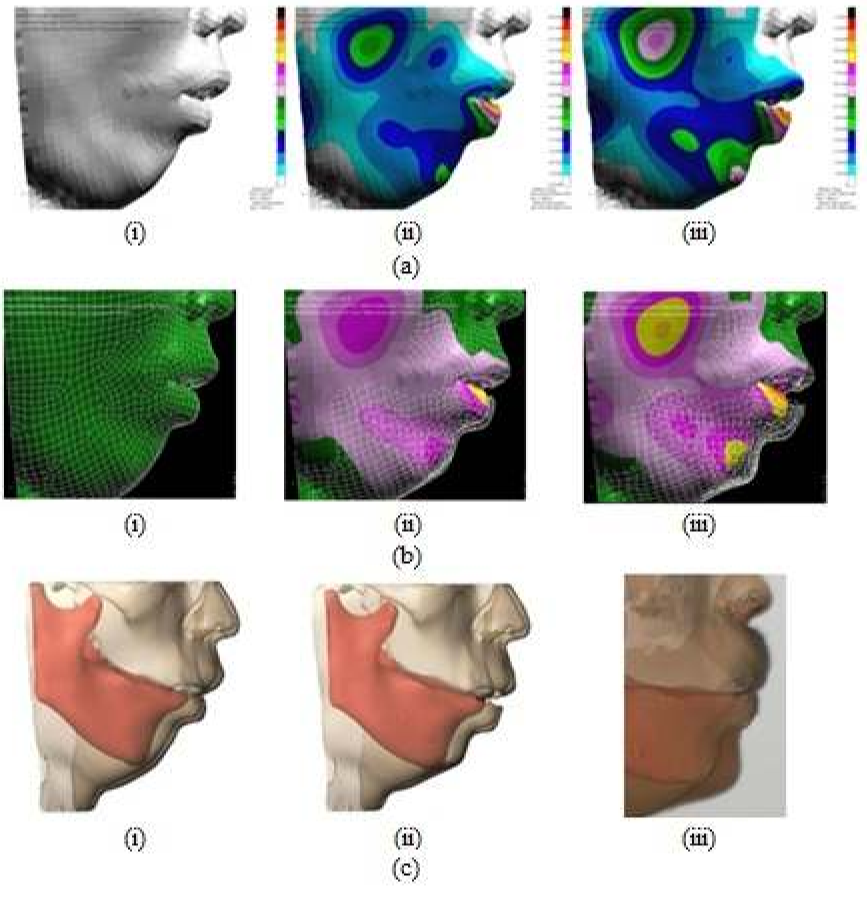

Fig 8: (a) The predicted facial appearance shown with incremental time steps where (i) 0 at an undeformed state, (ii) 40, and (iii) 55. (b) Simulation of the predicted postoperative facial appearance in (i) undeformed skin, (ii) the skin during simulation, and (iii) deformed skin. (c) Simulated prediction of postoperative appearance in (ii) based on available preoperative data in (i). The validation of the simulated and the actual postoperative picture is shown in (iii)

Finer deformation results were produced for higher element count. However, larger number of elements is computationally expensive. Thus, the total number of elements representing the models must be tolerable for the hardware specification. The second test verifies the theoretical and hypothetical deformable concept of the soft tissue where material property value for the skin was tested on a cylindrical model.

The result of the post operative appearance acquired from the finite element analysis simulated using the MSC.AFEA [45] on the discussed facial models is shown in Fig. 8 (a). These results were produced in terms of time steps where each increment of the time within a defined range produces slight deformation in an incremental order. The colours shown on the facial skin determines the stress distribution calculated throughout the simulation. Larger stress values are represented by hot colours such as red, orange and yellow, while the smaller values are signified by soft colours such as blue, green and pink. Fig. 8 (b) shows the general simulation of the soft tissue prediction using the wireframe option observing the difference between the undeformed and deformed states. An enhanced visual display is shown in Fig. 8 (c) (i) and (ii) of the preoperative and the simulated postoperative facial appearance.

The simulation results in time steps show variation of shape changes on the facial appearance. These variations are achieved through a few parameters such as stress, strain, deformation and displacement where each parameter interacts with each other to produce the predicted postoperative facial results. For example, for the deformation of facial skin under stress applied to a given region of the face our model can display the iterative variations of facial skin appearance at given time increments as shown in Fig. 8 (a).

The present results support the evidence that simulation of the finite element method using the contact analysis approach has the potential to accommodate the prediction of the postoperative appearance of an *orthognathic* surgery. This work also calls for further research particularly on the accuracy of the prediction by determining the most sensitive facial region requiring careful attention during the actual surgery. As the postoperative CT data is unavailable for this particular case, the quantitative validation is only performed by comparing the simulated results with the postoperative photograph of the respective patient. This evaluation shown in Fig. 8(c)(iii) is far from precision and error-prone. A better measurement may be derived by comparing with the actual post operative surgical CT data.

5.0 CONCLUSION

In this work, we proposed a general framework for the computer-assisted soft tissue prediction in an *osteotomy* surgery planning. The aesthetic surgery outcome is possible by the contact analysis of the finite element method. Our approach to individual prediction employs the patient-specific 3D facial models from the computer tomography data and the finite element method based on the realignment of underlying lower jaw producing the facial soft tissue deformations. Although the attributes of living tissues are complex, we assume linear elastic constitutive models based on the contact analysis model that proves to produce reasonable description of the soft tissue behaviour in predicting the patient-specific post operative appearance. These properties described the soft tissue behaviour such as elasticity, stiffness, thickness and density were incorporated and imposed on: (1) surface based quadrilateral models of the facial skin, (2) application of the displacement condition assigned to the selected elements to constraint the model from floating during computation, (3) assignment of forces to the bone model to represent the *osteotomy* (forward repositioning of the lower jaw) surgical procedures by employing the contact analysis between the facial skin and the underlying jaw model.

We are certain that the present method is promising given the positive feedback acquired from both craniofacial surgeons and the patients. The present findings offer further quantitative validation both computationally and clinically to develop the existing soft tissue models in order to provide an optimised solution for the post-operative surgical prediction with precise accuracy. The accuracy of the reported soft tissue simulation based on present surface based models can be improved by adopting volumetric models that consists of tetrahedral elements. Further development that strengthens the understanding of the constitutive models used to describe the soft tissues characteristics more accurately is equally important to produce reliable postoperative simulation results. This paper reported that the simulation of the facial soft tissue by means of the movement of the underlying bone through contact analysis is plausible. However, incorporating more soft tissue information such as the muscular anatomy in future work would also enable simulation of a more dynamic facial expression.

ACKNOWLEDGMENT

Special appreciation is conveyed to the Faculty of Dentistry, University of Malaya for providing data and information for this study.

REFERENCES

[1] W.C. Ngeow, S.T. Ong, K.K. Siow, C.B. Lian, "Orthognathic Surgery in the University of Malaya." *Medical Journal of Malaysia*, 2002, 57, pp. 398-403.

[2] K.E. Kahnberg, "Correction of Maxillofacial Asymmetry using Orthognathic Surgical Methods." *Journal of Cranio-Maxillofacial Surgery*, 1997, 25.5, pp. 254-260.

[3] J.F. Hoenig, "Sliding Osteotomy Genioplasty for Facial Aesthetic Balance: 10 years of Experience." *Aesthetic Plastic Surgery,* 2007, 31.4, pp. 384-391.

[4] D. Nicodemo, M. D. Pereira, & L. M. Ferreira, "Self-esteem and Depression in Patients Presenting Angle Class III Malocclusion Submitted for Orthognathic Surgery." *Medicina Oral Patologia Oral y Cirugia Bucal*, 2008, 13(1), 48.

[5] S. J. Cunningham, M. S. Gilthorpe, & N. P. Hunt, "Are orthognathic patients different?" *The European Journal of Orthodontics*, 2000, 22(2), pp. 195-202.

[6] W.H. Bell, J.D. Jacobs, & J.G. Quefada, "Simultaneous Repositioning of the Maxilla, Mandible, and Chin Treatment Planning and Analysis of Soft Tissues." *American Journal of Orthodontics*, 1986, 89(1), pp. 28-50.

[7] J. Xia, N. Samman, R. W. Yeung, D. Wang, S. G. Shen, H. H. Ip, & H. Tideman, "Computer-assisted Three-dimensional Surgical Planning and Simulation." *International Journal of Oral & Maxillofacial Surgery*, 2000, 29(4), pp. 250-258.

[8] R. Olszewski, M. B. Villamil, D. G. Trevisan, L. P. Nedel, C. M. Freitas, H. Reychler, & B. Macq, "Towards an Integrated System for Planning and Assisting Maxillofacial Orthognathic Surgery." *Computer Methods and Programs in Biomedicine*, 2008, 91(1), pp. 13-21.

[9] D. Terzopoulos and K. Waters, "Physically-based Facial Modeling, Analysis and Animation". *The Journal of* Visualization and Computer Animation, 1990, 1, pp. 73-80.

[10] H. H. S. Ip, C. S. Kot, & J. Xia, "Simulated Patient for Orthognathic Surgery." *in Computer Graphics International*, 2000, pp. 239-245.

[11] K. Kähler, J. Haber, & H. P. Seidel, "Geometry-based Muscle Modeling for Facial Animation." *in Graphics Interface*, 2001, pp. 37-46.

[12] J. Xia, H. H. S. Ip, N. Samman, H. T. Wong, J. Gateno, D. Wang, W.K.Y. Richie, S.B.K. Christy & H. Tideman, "Three-dimensional Virtual-reality Surgical Planning and Soft-tissue Prediction for Orthognathic Surgery." *Information Technology in Biomedicine*, 2001, 5(2), pp. 97-107.

[13] E. Keeve, S. Girod, B. Girod, "Computer-aided Craniofacial Surgery." *Computer Assisted Radiology (CAR)*, 1996, 3(2), pp. 66-70.

[14] R.M. Koch, M.H. Gross, F.R. Carls, D.F. von Büren, G. Fankhauser, Y.I.H. Parish, “Simulating Facial Surgery using Finite Element Models.” *in SIGGRAPH’96 Conference Proceedings, Annual Conference Series, ACM SIGGRAPH*, 1996, 4(9), pp. 421-428.

[15] S. Zachow, E. Gladilin, H.-C. Hege, P. Deuflhard, “Finite-element Simulation of Soft Tissue Deformation.” *Proceedings of the 14th International Symposium: Computer Assisted Radiology and Surgery,* 2000, 14, pp. 23–28.

[16] R.M Koch. *Methods for Physics Based Facial Surgery Prediction*. Ph.D. diss., Department of Computer Science, ETH Zürich, 2000.

[17] E. Gladilin, S. Zachow, P. Deuflhard, H.-C. Hege, “A Biomechanical Model for Soft Tissue Simulation in Craniofacial Surgery”. *in Proc. of MIAR*, 2001, pp. 137-141.

[18] J.G. Schmidt, G. Berti, J. Fingberg, J. Cao, G. Wollny, “A Finite Element based Tool Chain for the Planning and Simulation of Maxillo-facial Surgery.” *In Proc. of European Congress on Computational Methods in Applied Sciences and Engineering, ECCOMAS*, 2004, pp. 1-17.

[19] W. Maue-Dickson, M. Trefler and D.R. Dickson. “Comparison of Dosimetry and Image Quality in Computed and Conventional Tomography”. *J. of Radiology*, 1979, 131, pp. 509-514.

[20] A. Shirkhoda, H.R. Brashear, M.E. Zelenik, D.C. Burke, “Sacral Abnormalities--Computed Tomography versus Conventional Radiography.” *J Comput. Tomogr*, 1984, 8(1), pp. 41-51.

[21] A. Kawamata, Y. Ariji, R.P. Langlais, “Three-dimensional Computed Tomography Imaging in Denstistry.” *Dental Clinics of North America*, 2000, 44, pp. 395-410.

[22] D.C. Hemmy, D.J. David, G.T. Herman, “Three-dimensional Reconstruction of Craniofacial Deformity using Computer Tomography.” *Neurosurgery*, 1983, 13, pp. 534-541.

[23] B.L. Daniel, S.S. Jeffery, R.L. Birdwell, D.M. Ikeda, A.M. Sawyer-Glover, R.J. Herfkens. “Three-dimensional Shaded-surface Rendering of MR Images of the Breast: Technique, Applications and Impact on Surgical Management of Breast Disease.” *Radiographics*, 1998, 18, pp. 483-496.

[24] V. M. Nastri, P.S. L. Baptista, Baroni, H. Ronaldo, R. Blasbalg, L.F. de Ávila, C.C. Leite, C.C. de Castro, G.G. Cerri, “Gadolinium-enhanced Three-dimensional MR Angiography of Takayasu Arteritis.” *Radiographics*, 2004, 24, pp. 773-786.

[25] A. Delcker and H.C. Diener, “Quantification of Atherosclerotic Plaques in Carotid Arteries by Three-dimensional Ultrasound.” *The British Journal of Radiology*, 1994, 67, pp. 672-678.

[26] A. M. Aisen, W. Martel, E. M. Braunstein, K. I. McMillin, W. A. Phillips, & T. F. Kling, “MRI and CT Evaluation of Primary Bone and Soft-tissue Tumors.” *American Journal of Roentgenology*, 1986, 146(4), pp.749-756.

[27] M.W. Vannier, J.L. Marsh, J.O. Warren, “Three Dimensional Computer Graphics for Craniofacial Surgical Planning and Evaluation.” *Computer Graphics,* 1983, 17(3), pp. 263-273.

[28] T. Yasuda, Y. Hashimoto, S. Yokoi, J. Toriwaki, “Computer System for Craniofacial Surgical Planning based on CT Images”. *IEEE Transactions on Medical Imaging,* 1990, *9(3)*: 270-280.

[29] J. Xia, F. Qi, W. Yuan, D. Wang, W. Qiu, Y. Sun, Y. Huang, G. Shen, H. Wu, “Computer Aided Simulation System for Orthognathic Surgery”. *Proceedings of Eight IEEE Symposium on Computer-based Medical Systems, IEEE Computer Society Press.,* 1995, 11, pp. 386-393.

[30] M. Teschner, S. Girod, B. Girod, "Interactive Osteotomy Simulation and Soft-tissue Prediction". *in Proc Vision, Modeling and Visualization, VMV'99,* 1999, pp. 405-412.

[31] Y. Lee, and D. Terzopoulos, "Realistic Modeling for Facial Animation." *Proceedings of SIGGRAPH '95, Computer Graphics Proceedings, Annual Conference Series*, 1995, pp. 55-62.

[32] L.P. Nedel and D. Thalmann, "Real Time Muscle Deformations using Mass-spring Systems." *Computer Graphics International*, 1998, pp. 156-165.

[33] D. Bourguignon and M.-P. Cani, "Controlling Anisotropy in Mass-spring Systems." *Computer Simulation and Animation*, 2000, pp.113-123.

[34] K. Waters, J. Frisbie, "A Coordinated Muscle Model for Speech Animation." *Proceeding of Graphics Interface 95*, 1995, pp. 163-170.

[35] S.F.F. Gibson, and B. Mirtich, *A survery of deformable modeling in computer graphics*. Technical Report TR-97-19, Mitsubishi Electric Research Laboratory, Cambridge, MA, USA, 1997.

[36] E. Keeve and R. Kikinis, "Deformable Modeling of Facial Tissue". *Proceedings of the First Joint BMES/EMBS Conference Serving Humanity, Advancing Technology*, 1999, 502.

[37] H. Delingette, "Toward realistic soft-tissue modeling in medical simulation." *Proc. of IEEE : Special Issue on Surgery Simulation*, 1998, 86(3), pp. 512-523.

[38] S.D. Pieper. *CAPS: Computer-aided plastic surgery*. Ph.D. diss., MIT, Media Arts and Sciences, Cambrigde, MA, 1991.

[39] R.M. Koch, S.H.M. Roth, M.H. Gross, A.P. Zimmermann, H.F. Sailer, "A framework for facial surgery simulation". *Proceedings of ACM Spring Conference on Computer Graphics,* 2002.

[40] S. Zachow, Th. Hierl, B. Erdmann, "A quantitative evaluation of 3D soft tissue prediction in maxillofacial surgery planning". *in Proc. 3 Jahrestagung der Deutschen Gesellschaft für Computer-und Roboter-assistierte Chirurgie(CURAC),* 2004, 3, pp. 75-79.

[41] H. Kim, P. Jürgens, M. Reyes, "Soft-Tissue Simulation for Cranio-Maxillofacial Surgery: Clinical Needs and Technical Aspects." *Patient-Specific Modeling in Tomorrow's Medicine*, 2012, pp. 413-440.

[42] W.E. Lorensen, H.E. Cline. "Marching cubes: A High Resolution 3D Surface Construction Algorithm." *SIGGRAPH 1987, ACM Computer Graphics 21*, 1987, pp. 163-169.

[43] Materialise. *Mimics 8.1 Software.* Belgium, 1991.

[44] Y.C. Fung. *Biomechanics: Mechanical Properties of Living Tissues*. Springer, New York, 1993.

[45] MSC.Software Corporation. *MSC.AFEA software*. Santa Ana, USA, 1999.